TiF1-Gamma Plays an Essential Role in Murine Hematopoiesis and Regulates Transcriptional Elongation of Erythroid Genes

Citation

Published Version

Permanent link

http://nrs.harvard.edu/urn-3:HUL.InstRepos:12582487

Terms of Use

Share Your Story

NIH-PA Author Manuscript

TIF1-GAMMA PLAYS AN ESSENTIAL ROLE IN MURINE HEMATOPOIESIS AND REGULATES TRANSCRIPTIONAL ELONGATION OF ERYTHROID GENES

Xiaoying Bai[1,2,3,*,§], **Jennifer J. Trowbridge**[2,3,4,*,¶], **Elizabeth Riley**[1,2,3], **Joseph A. Lee**[1,2,3], **Anthony DiBiase**[1,2,3], **Vesa M. Kaartinen**[6], **Stuart H. Orkin**[2,3,4,5], and **Leonard I. Zon**[1,2,3,4,5,7]

[1]Stem Cell Program, Children's Hospital Boston, Boston, MA 02115, USA

[2]Division of Hematology/Oncology, Children's Hospital Boston, Boston, MA 02115, USA

[3]Harvard Stem Cell Institute, Harvard Medical School, Boston, MA 02115, USA

[4]Department of Pediatric Oncology, The Dana Farber Cancer Institute, Boston, MA 02115, USA

[5]Howard Hughes Medical Institute, University of Michigan, Ann Arbor, MI 48109, USA

[6]Department of Biologic and Materials Sciences, School of Dentistry, University of Michigan, Ann Arbor, MI 48109, USA

Abstract

Transcriptional regulators play critical roles in the regulation of cell fate during hematopoiesis. Previous studies in zebrafish have identified an essential role for the transcriptional intermediary factor TIF1γ in erythropoiesis through regulating the transcription elongation of erythroid genes. To study if TIF1γ plays a similar role in murine erythropoiesis and to assess its function in other blood lineages, we generated mouse models with hematopoietic deletion of TIF1γ. Our results showed a block in erythroid maturation in the bone marrow following *tif1γ* deletion that was compensated with enhanced spleen erythropoiesis. Further analyses revealed a defect in transcription elongation of erythroid genes in the bone marrow. In addition, loss of TIF1γ resulted in defects in other blood compartments, including a profound loss of B cells, a dramatic expansion of granulocytes and decreased HSC function. TIF1γ exerts its functions in a cell-autonomous manner as revealed by competitive transplantation experiments. Our study therefore demonstrates that TIF1γ plays essential roles in multiple murine blood lineages and that its function in transcription elongation is evolutionarily conserved.

Keywords

Hematopoiesis; lineage differentiation; transcription elongation

Introduction

Differentiation from a single hematopoietic stem cell (HSC) to mature blood cells comprised of all hematopoietic lineages is tightly regulated by the interplay between external signals and internal nuclear factors(Orkin and Zon, 2008). In addition to cell type-specific transcription factors, general transcription factors and co-factors play equally important roles in gene regulation. The transcriptional co-factor Transcriptional Intermediary Factor 1 gamma (TIF1γ, also known as TRIM33/RFG7/PTC7/Ectodermin) has been shown to play an essential role in erythroid differentiation(Bai et al., 2010; He et al., 2006; Ransom et al., 1996). TIF1γ was first identified by sequence homology to two other TIF1 family members, TIF1α and β(Venturini et al., 1999). The TIF1 family members are characterized by a N-terminal RBCC or TRIM domain(Reymond et al., 2001)composed of a RING finger, two B-boxes, and a coiled-coil domain, and the C-terminal PHD finger and bromodomain. Loss of TIF1γ function in the zebrafish *moonshine(mon)* mutant causes a rapid loss of erythroid gene expression, leading to a profound anemia and embryonic lethality(Ransom et al., 2004).

We previously conducted a genetic suppressor screen using *mon* mutants and identified an important role for TIF1γ in transcription elongation of RNA polymerase II (Pol II) on erythroid genes. Recent genome-wide studies identify transcription elongation as a major rate-limiting step in gene regulation(Guenther et al., 2007; Muse et al., 2007; Zeitlinger et al., 2007). After the initiation of transcription, Pol II often pauses at the proximal promoter of many genes due to the presence of pausing factors DSIF and NELF(Wu et al., 2003; Yamaguchi et al., 2002). To release Pol II, the C-terminal domain (CTD) of the large subunit of Pol II needs to be converted from serine5-phosphorylation to serine2-phosphorylation. This process is regulated by the p-TEFb kinase complex and other positive elongation factors(Cheng and Price, 2007; Peterlin and Price, 2006). Our previous study identified zebrafish genetic mutants rescuing *mon* by affecting Pol II pausing(Bai et al., 2010). Together with the biochemical data, our model suggests that TIF1γ physically interacts with the SCL transcription complex in erythroid cells and recruits the positive elongation factors p-TEFb and the FACT complex to eythroid genes to release paused Pol II.

In the current study, we investigated whether the function of TIF1γ is conserved in murine erythropoiesis and whether TIF1γ has other roles in hematopoiesis and HSC function. Since embryonic deletion of *tif1γ* leads to early lethality(Kim and Kaartinen, 2008), we generated conditional knockouts of TIF1γ in the mouse hematopoietic system using both Mx-cre and vav-cre. We have found that TIF1γ plays important roles in the B cell and granulocyte lineages, as well as in HSCs. Our results also demonstrate defective bone marrow erythropoiesis in the murine TIF1γ knockout. Analyses on bone marrow erythroid cells review a significant reduction in elongation-engaged Pol II (Ser2-P Pol II) in the absence of TIF1γ and a specific decrease of the 3' transcript levels of several erythroid genes. The genetic data, coupled with the analysis of gene transcription, establishes TIF1γ as a major regulator of transcription elongation in erythroid cells, and supports our previous conclusions from the zebrafish.

Materials and Methods

Experimental Animals

TIF1γ^fl/fl mice, Mx-Cre transgenic mice and vav-cre mice were maintained on a C57BL/6 background. pI-pC (Sigma) was administered via i.p. injection at a dose of 25 μg/kg. To confirm deletion of TIF1γ, genomic DNA was extracted from fetal liver or whole bone

marrow (BM) and PCR genotyped with described primers(Kim and Kaartinen, 2008). The Children's Hospital Boston Animal Ethics Committee approved all experiments.

Flow Cytometry Analysis

Single-cell suspensions of bone marrow were prepared from pooled femurs, tibiae, and iliac crests, and peripheral blood (PB) was isolated via the retro-orbital plexus. Whole PB differential counts were determined with an AcT 10 analyzer (Beckman Coulter). RBCs were lysed with ammonium chloride buffer prior to staining. Fluorochrome-conjugated antibody clones were obtained from eBioscience: Gr-1 (RB6-8C5), CD11b (M1/70), F4/80 (BM8), IgM (II/4I), CD43 (S7), B220 (RA3-6B2), CD71 (R17217), Ter-119, CD4 (GK1.5), CD8a (53-6.7). Flow cytometric analysis was performed on a FACSCalibur (Becton Dickinson, BD) and all data were analyzed with FlowJo (Tree Star, Inc.).

Analysis of Hematopoietic Stem and Progenitor Cells

Lineage depletion of BM, spleen, or PB cells from control or $TIF1\gamma^{\Delta/\Delta}$ mice was performed as described by the manufacturer (Dynabeads Sheep anti-Rat IgG, Invitrogen) with affinity-purified rat anti-mouse antibodies (eBioscience) against CD3, CD4, CD5, CD8a, B220, Gr-1, CD11b, Ter119. Lineage-depleted cells were stained with fluorochrome-conjugated antibodies (eBioscience) recognizing CD117 (c-Kit; 2B8), Sca-1 (E13-161.7), CD34 (RAM34), CD16/CD32 (FcγIII/II Receptor; 2.4G2), and CD127 (IL-7Rα; A7R34) and analyzed on a LSRII (BD). Colony-forming unit (CFU) assays were performed by plating spleen cells into MethoCult SF M3436 (StemCell Technologies) and scoring BFU-E colonies after 10 days.

Competitive Bone Marrow Transplantation Analysis

BM cells from *Mx-cre; tif1$\gamma^{fl/fl}$* or *Mx-cre; tif1$\gamma^{+/+}$* (CD45.2$^+$) were co-injected retro-orbitally with BM cells from CD45.1$^+$ competitors at a ratio of 1:1 (1×10^6 cells each) into congenic female C57BL/6 (CD45.1$^+$) mice (The Jackson Lab). pI-pC (Invivogen) was administered at 3-week posttransplent via i.p. injection at a dose of 25 μg/kg. The PB chimerism of recipient mice was assessed with fluorochrome-conjugated antibodies against CD45.1 (A20), CD45.2 (104) (eBioscience), and multilineage antibodies as described. Donor cell engraftment was determined at 18 weeks posttransplant.

Global Gene Expression Analysis

Purified Lin$^-$ Sca-1$^-$ c-Kit$^+$ CD34$^+$ CD16/32^{hi} GMPs from individual mice (three replicates) were isolated by FACSAria (BD) from control or *tif1$\gamma^{\Delta/\Delta}$* mice. Total RNA was extracted with the RNeasy Micro Kit (QIAGEN), treated with DNaseI, reverse transcribed, and amplified with the WT-Ovation Pico RNA Amplification System (NuGEN Technologies). Single-stranded cDNA amplification products were purified with QIAquick PCR Purification Kit (QIAGEN) and labeled with the FL-Ovation cDNA Biotin Module V2 (NuGEN). Hybridization to GeneChip Mouse Genome 430A 2.0 Arrays (Affymetrix), washing, and scanning were performed by the CHB Microarray Core Facility (Boston, MA). The golden spike package in Bioconductor/R(Choe et al., 2005) was used to process CEL files. Independent biological repeats were combined by averaging the signal intensities of each probe represented on the microarray. Probes with an averaged signal intensity of >100 from at least one of the repeats were further analyzed (a total of 8723 probes). All microarray data have been deposited to GEO and will be available to public upon acceptation of the manuscript.

Quantitative Real-Time PCR

RNA was isolated from purified CD71^{hi}Ter119^{+} cells with the RNeasy Micro Kit (QIAGEN) and treated with DNaseI prior to reverse transcription. cDNA was prepared with SuperScript III (Invitrogen). Quantitative real-time PCR was performed with iQ SYBR Green mix (Bio-Rad) on an iCycler (Bio-Rad) and Ct values were normalized to β-actin levels.

Primers for 5' transcripts:

β-actin-F: 5-cagcttctttgcagctcctt-3

β-actin-R: 5-acgatggaggggaatacag-3

gata1-F: 5-gaatcctctgcatcaacaagc-3

gata1-R: 5-aacctgtggaatctgatggtg-3

scl-F: 5-gacctcacggcaagctaagta-3

scl-R: 5-gagagacctactcggctggtt-3

hba-F: 5-gctctctggggaagacaaaag-3

hba-R: 5-gggaagctagcaaacatcctt-3

eklf-F: 5-atagcccatgaggcagaaga-3

eklf-R: 5-cctgggtgtccagaaactgt-3

gfi-1b-F: 5-gccacggtcctttctagtga-3

gfi-1b-R: 5-tgccacaggaattacagcag-3

Primers for 3' transcript:

β-actin-F: 5-acattggcatggctttgttt-3

β-actin-R: 5-gtttgctccaaccaactgct-3

gata1-F: 5-ataagggtgaccccacatttc-3

gata1-R: 5-aacaacaaaccccacaaaaca-3

scl-F: 5-ggcagacagagactgatcctg-3

scl-R: 5-aatgggaaagaaccagcctta-3

hba-F: 5-aaattccttgcctctgtgagc-3

hba-R: 5-aggtgcaagggagagaagaag-3

eklf-F: 5-gagtggatccaaggaccgta-3

eklf-R: 5-ccctgaggacatgtgaggtt-3

gfi-1b-F: 5-ttcaatgccagagcacagac-3

gfi-1b-R: 5-acccagagaagcaagcaaga-3

Statistical Analyses

Statistical analyses were performed with unpaired Student's t tests.

Western Blot Analysis

Purified CD71^{hi}Ter119^{+} cells from control or *tif1γ*$^{Δ/Δ}$ mice were pooled (2 mice each group) and whole-cell lysates were separated by SDS-PAGE. Proteins were detected by the following antibodies: anti-pol2-S2 (Pol II H5 antibody, Covance), anti-Pol2-S5 (Abcam ab5131), anti-pol2 (N-20, Santa Cruz) and anti-TBP (Abcam).

Histological analyses

Spleen and liver tissues from *vav-cre*; *tif1γ*$^{fl/fl}$ mice were fixed for 24 h in 10% buffered formalin, dehydrated and embedded in paraffin. Paraffin blocks were sectioned at 5 mm and stained with haematoxylin and eosin.

Results

Bone marrow erythroid differentiation is blocked by *TIF1γ* deletion and can be compensated by spleen erythropoiesis

To study the role of TIF1γ in murine hematopoiesis, we induced *tif1γ* excision in the mouse hematopoietic system via interferon-mediated Cre expression by mating *tif1γ*$^{fl/fl}$ mice with Mx-cre mice. In this model, Cre expression and subsequent deletion of *tif1γ* is induced by injection of polyI-polyC (pI-pC)(Kuhn et al., 1995). Analysis of peripheral blood at 3 weeks post-injection revealed a modest increase in CD71^{+}Ter119^{+} immature erythroid cells in TIF1γ-deficient mice compared to control mice (*Mx-cre*; *tif1γ*$^{fl/+}$), suggesting a possible blockage of erythroid differentiation (supplemental fig.1A). This was further confirmed by FACS analysis of bone marrow, where we observed an increase of c-Kit^{hi}CD71^{+}Ter119^{-} cells that morphologically similar to the early erythroid progenitors (supplemental fig.1C), and a decrease in more differentiated erythroid progenitors, including the CD71^{hi}Ter119^{hi} R2 population, in TIF1γ-deficient mice (Fig. 1A). Genomic PCR analyses confirmed deletion of *tif1γ* in Mx-cre; *tif1γ*$^{fl/fl}$ bone marrow (BM) cells (supplemental fig.1B). Interestingly, analysis of the spleens of TIF1γ-deficient mice revealed enhanced erythropoiesis at multiple stages of differentiation (Fig. 1B). Consistent with this *in vivo* data, BFU-E colony assays using isolated spleen cells revealed an almost 10-fold increase in BFU-E formation from TIF1γ-deficient cells compared to control cells (Fig. 1C).

To study the role of TIF1γ during hematopoietic development, we generated an additional conditional knockout model using vav-cre. Vav-cre deletion, which is restricted to blood cells, initiates at E11.5 in the fetus and induces cre-mediated gene deletion in all definitive blood lineages throughout hematopoietic development(Ogilvy et al., 1999). Vav-cre; *tif1γ*$^{fl/fl}$ mice were born at a normal Mendelian ratio and FACS analysis of E14.5 fetal liver failed to detect any defects in erythropoiesis (Supplemental fig.1D). Genomic PCR analysis detected the presence of both unexcised and excised *tif1γ* alleles in the vav-cre; *tif1γ*$^{fl/fl}$ fetal liver cells (Supplemental fig.1E), suggesting that the lack of phenotype may be caused by incomplete excision of *tif1γ* at this early stage. In contrast, bone marrow analysis of 12 to 14-week old adult mice showed complete deletion of *tif1γ* in *vav-cre; tif1γ*$^{fl/fl}$ BM cells (data not shown) and revealed a profound defect in erythroid differentiation. We observed significant decreases in the R2 and R3 stages of erythroid progenitors, while the c-Kit^{hi}CD71^{+}Ter119^{-} early erythroid progenitors and R1 stages were increased in *tif1γ*-deficient mice (Fig 1D). This block in erythroid differentiation was more severe than that observed in *Mx-cre; tif1γ*$^{-/-}$ mice. Furthermore, spleen erythropoiesis was also enhanced in the vav-cre; *tif1γ*$^{fl/fl}$ mice, similar to that observed in Mx-cre; *tif1γ*$^{fl/fl}$ mice (Fig. 1E).

Enhanced splenic erythropoiesis is generally viewed as a stress response when bone marrow erythroid cell production is insufficient. A key regulatory pathway of this process is BMP4-Smad5. To test if stress erythropoiesis is activated in TIF1γ-deficient mice, we analyzed the

level of phosphorylated Smad5 protein in spleen erythrocytes. As shown in Figure 1F, we observed a clear increase of Smad5 phosphorylation in R2-stage erythroidcells from TIF1γ-deficient spleen. On the other hand, no changes in the transcription level of a selective set of erythroid genes were detected in these cells (Fig. 1G), suggesting that there is no acceleration of erythroid differentiation in spleen. These data thus suggest that TIF1γ is required for BM erythropoiesis and that extramedullary erythropoiesis in the spleen is activated to compensate for this defect likely through regulating cell proliferation.

Other lineage defects caused by TIF1γ deficiency

In addition to erythroid defects, we also observed B cell and myeloid defects in TIF1γ-deficient mice. Loss of B cells was seen as early as 1 week post-injection of pI-pC in the *Mx-cre*; *tif1γ*^fl/fl mice (Fig. 2A). Both BM and spleen analyses at 3 weeks post-injection revealed a dramatic decrease in pre-B (CD43$^-$ B220$^+$ IgM$^-$) and mature/immature B cells (CD43$^-$ B220$^+$ IgM$^+$) in the TIF1γ-deficient mice, whereas the number of pro-B cells (CD43$^+$ B220$^+$ IgM$^-$) remained relatively normal (Fig. 2B). Similar defects were also detected in the vav-cre; *tif1γ*^fl/fl mice (supplemental fig.2A). Gene expression analyses by quantitative RT-PCR showed no change of transcription levels of several key regulatory genes for B-cell differentiation and function, including *E2A, Ebf1, Pax5* and *Rag1* (Fig. 2C), suggesting that the loss of B cells is not caused by a differentiation blockage. Because we observed a relatively rapid loss of B cells in Mx-cre induced TIF1γ-KO mice, we analyzed the expression of genes involved in apoptosis, including *pten* and *p53*. Quantitative RT-PCR showed a significant upregulation of *pten* expression in pro-B cells, followed by a similar increase of *p53* transcription in pre-B cells (Fig. 2C). These data therefore suggest that increased apoptosis is the major cause of B-cell loss in TIF1γ-deficient mice.

In contrast to the loss of B cells, an increase in myeloid cells (Gr1$^+$ Mac1$^+$) was observed in both Mx-cre and vav-cre-induced TIF1γ-deficient mice (Fig. 2A, 3A and supplemental fig. 2A), suggesting a negative role for TIF1γ in regulating the myeloid lineage. Remarkably, ~40% of vav-cre; *tif1γ*^fl/fl mice died before 6 months of age with dramatically increased myeloid cells in the peripheral blood and splenomegaly (Fig. 3B). Wright–Giemsastaining showed that these cells were mainly differentiated granulocytes (Fig. 3C). Histological analysis of the spleen and liver showed a marked infiltration by myeloid cells(Fig. 3C). Taken together, these findings represent diagnostic criteria for a myeloproliferative/myelodysplastic process and reminiscent of human chronic myelomonocytic leukemia (CMML)(Emanuel, 2008), suggesting that TIF1γ has a tumor suppressor role in the myeloid lineage.

TIF1γ deficiency leads to increase in GMPs

We then analyzed the frequency of bone marrow progenitors and HSCs in the TIF1γ-deficient mice by FACS analysis. We observed an increase in granulocyte-macrophage progenitors (GMPs) in both Mx-cre and Vav-cre-induced TIF1γ-deficient mice (Fig.4A and Supplemental fig. 2 B). To begin to understand the molecular changes underlying the increase in GMPs, we sorted GMP cells and performed microarray analyses to compare transcriptional profiles between TIF1γ-deficient and control GMPs. Among 282 downregulated genes (q=0.005) in TIF1γ-deficient GMPs, we found multiple genes related to erythroid cell fate, such as globin, gata1 and EKLF (Fig. 4B). In contrast, genes representative of the myeloid signature(Klinakis et al., 2011), including myeloid-fate regulators CEBP-α, CEBP-β and CEBP-δ, were found to be upregulated (Fig. 4B). These data are consistent with the essential function of TIF1γ in erythroid gene transcription and suggest that lack of TIF1γ may promote cell fate towards the myeloid lineage.

Cell-autonomous effect of TIF1γ

Interestingly, we observed a trend of increase in the frequencies of multipotent progenitors (MPPs), short-term (ST)-HSCs and long-term (LT)-HSCs in TIF1γ-deficient mice as defined by surface marker expression(Fig. 4C and Supplemental fig. 2C). To test if TIF1γ alters HSC function in a cell-autonomous fashion, we performed competitive transplantation assays (Fig. 5A). To bypass any potential homing defects in the TIF1γ-deficient cells, we used *Mx-Cre; tif1γ*$^{fl/fl}$ donors and induced *tif1γ* excision after transplantation by pI-pC injection. Whole BM cells from CD45.2$^+$ *Mx-cre*; *tif1γ*$^{fl/fl}$ donors or control donors (*Mx-Cre tif1γ*$^{+/+}$) were mixed at a 1:1 ratio with CD45.1$^+$ whole BM cells from wild-type competitor mice and transplanted into lethally irradiated CD45.1$^+$ recipients. At 3 weeks post-transplantation, peripheral blood analyses of the recipients revealed comparable chimerism of CD45.2$^+$ cells from the Mx-cre; *tif1γ*$^{fl/fl}$ donors and control donors (*Mx-Cre*; *tif1γ*$^{+/+}$) (supplemental fig. 3A). Injection of pI-pC was then performed to induce *tif1γ* excision *in Mx-cre*; *tif1γ*$^{fl/fl}$ donor-derived cells. One week after pI-pC, the number of CD45.2$^+$ cells in the peripheral blood from TIF1γ-deficient donors was reduced (Fig. 5B). Noticeably, TIF1γ-deficient-donor derived CD45.2$^+$ cells were found to have an increased contribution to the myeloid lineage and decreased contribution to the B cell lineage, resembling the phenotype of the non-transplanted TIF1γ-deficient mice. This pattern of chimerism was maintained for 18 weeks at which time the recipient mice were sacrificed for BM analysis (supplemental fig. 3B). These data are consistent with a long-term deficit in the ability of TIF1γ-deficient cells to contribute to proper hematopoiesis. A similar B-cell and myeloid chimerism pattern was seen in the BM of mice that received Mx-cre; *tif1γ*$^{fl/fl}$ cells (Fig. 5C), together suggesting a cell-autonomous role of TIF1γ in these lineages.

At the level of progenitors, TIF1γ-deficient donor cells made a significantly greater contribution to GMPs, again phenocopying the non-transplanted TIF1γ-deficient mice. In contrast, the contribution to megakaryocyte-erythroid progenitors (MEPs) by TIF1γ-deficient donor cells was profoundly reduced compared to control (Fig. 5D), suggesting a cell-autonomous function of TIF1γ in promoting the erythroid lineage fate. Interestingly, although TIF1γ-deficient mice tended to have an increased number of phenotypic HSCs (Fig. 4C), we detected a reduced contribution to the recipient LT-HSC compartment by TIF1γ-deficient donor cells upon transplantation (Fig. 5E), suggesting reduced HSC function. These data implicate TIF1γ in control of normal HSC function, including proper differentiation to mature hematopoietic lineages.

Transcription elongation is defective on TIF1γ-deficient erythroid genes

Our previous work had identified an important function of TIF1γ in transcription elongation of erythroid genes in zebrafish(Bai et al., 2010). To study if this function is conserved in murine erythropoiesis, we purified the R2 stage (CD71^{hi} Ter119$^+$) of erythroid progenitors from *vav-cre; tif1γ*$^{fl/fl}$ mice and control mice. We first performed quantitative RT-PCR on several erythroid genes to compare the relative amount of transcripts at either the 5' end or 3' end using gene-specific primers targeting either mature RNA or nascent transcripts(Fig. 6A and supplemental fig. 4). When compare TIF1γ-deficent erythroidcells with control cells, we detected either unchanged (*gata1, eklf and gfi-1b*) or increased transcript level (*scl, hba*) at the 5' end, whereas the levels of 3' transcripts were significantly reduced for all tested erythroid genes (Fig. 6A). No such changes were detected on the control gene *b-actin*. These data are consistent with our model that TIF1γ regulates the Pol II elongation of erythroid genes.

Transcription elongation is marked by a transition from serine 5-phosphorylated Pol II (S5-P Pol II) to serine 2-phosphorylated Pol II (S2-P Pol II)(Wada et al., 1998). The amount of S2-P Pol II is therefore correlated with overall elongation activity within cells. To test if TIF1γ

regulates overall transcription elongation in erythroid cells, we performed western blot analysis on isolated CD71^{hi}Ter119$^+$ (R2) erythroid cells using a specific antibody recognizing S2-P Pol II. As shown in Fig. 6B, a clear reduction of S2-P Pol II protein level was detected in TIF1γ-deficient cells while no significant change was detected for the levels of total Pol II or S5-P Pol II in the same cells. The normal level of S5-P Pol II level suggests that proper initiation of transcription of erythroid genes can occur in the absence of TIF1γ; however, transcription elongation of these genes may be blocked, as suggested by the reduced S2-Pol II level.

Discussion

Evolutionarily conserved function of TIF1γ in Pol II elongation of erythroid genes

TIF1γ has been shown to play a critical role in erythropoiesis in both zebrafish and human cell culture models.[2–4] In the present study, we investigated whether TIF1γ plays a similar role in regulating the transcriptional elongation of erythroid genes in murine hematopoiesis. We found a significant reduction in elongation-engaged Pol II (Ser2-P Pol II) in TIF1γ KO erythroid cells together with a specific decrease in 3' transcripts of several erythroid genes, demonstrating defective Pol II elongation in these cells in the absence of TIF1γ.

Using the mouse as a model system allows for dissection and examination of the intricate erythroid maturation process through the use of stage-specific surface markers. Loss of TIF1γ leads to an accumulation of the c-Kit^{hi}CD71$^+$ Ter119$^-$ erythroid progenitors and a subsequent reduction in the more differentiated R2 and R3 populations, suggesting that TIF1γ is required for erythroid maturation from a very early stage, possibly immediately following the initial commitment to the erythoid cell fate. These findings are consistent with the zebrafish *moonshine* mutant phenotype where a decrease in gata1 expression was seen as early as the 11–12 somite stage(Ransom et al., 2004).

Differential response of BM and spleen erythroid progenitors to loss of TIF1γ

Loss of TIF1γ in the zebrafish *moonshine* mutant results in a profound loss in both primitive and definitive erythroid cells, providing the first evidence that TIF1γ is required for vertebrate erythropoiesis(Ransom et al., 2004). Subsequent RNAi knockdown studies of TIF1γ in human CD34+ cells revealed a block in erythroid differentiation in a TGF-β-dependent manner(He et al., 2006). Based on these findings, our observation that the loss of TIF1γ in the murine hematopoietic system did not cause severe anemia was surprising. Further analyses indicated that BM erythropoiesis was indeed affected but was compensated for by enhanced spleen erythropoiesis. Accelerated spleen erythropoiesis is typically viewed as a stress response to maintain homeostasis of red blood cell mass when acute or chronic loss of red blood cells occurs(Paulson et al., 2011). It is known that the BMP-Smad5 signaling pathway plays a central role in initiating this stress response(Porayette and Paulson, 2008). Interestingly, TIF1γ has been suggested to antagonize BMP signaling though Smad4 ubiquitination(Dupont et al., 2005). Thus, it is possible that the absence of TIF1γ may trigger BMP signaling which in turn induces stress erythropoiesis in spleen that compensates the erythroid defect in mouse bone marrow. Indeed, we have found an increase of Smad5 phosphorylation in spleen erythroid cells following TIF1γ deletion, indicating the activation of stress erythropoiesis.

Our finding that loss of TIF1γ does not alter the transcription of erythroid genes in spleen cells suggests that transcription elongation of erythroid genes can occur in certain situations independent of TIF1γ. It is possible that a signal transduction event, perhaps during stress-induced erythropoiesis, can bypass the block to transcription elongation caused by TIF1 γ deficiency. A potential candidate involved in recruitment of the elongation machinery is

Smad5. It has been shown recently by Alarcon et al that Smad1/5 can be phosphorylated by CDK9(Alarcon et al., 2009), the kinase in the p-TEFb complex. It is possible that BMP-Smad signaling pathway is involved in regulating Pol II elongation.

TIF1γ regulates cell fate of other blood lineages and HSC function

Using both Mx-cre and vav-cre-induced deletion of *tif1γ*, we found multi-lineage defects in TIF1γ-deficient mice. Similar phenotypes were recently reported utilizing a distinct conditional KO model of TIF1γ(Kusy et al., 2011). Together these results demonstrate the requirement for TIF1γ in multiple blood lineages and differentiation stages during murine hematopoiesis. The most profound blood defects in the TIF1γ-deficient mice reside in the B cell and myeloid lineages. A loss of B cells and increase in myeloid cells were detected in the peripheral blood as early as one-week post–deletion of *tif1γ*. The rapid loss of B cells correlates with anupregulation of apoptotic genes *pten* and *p53* in TIF1γ-deficient B-cell progenitors, suggesting enhanced cell death as the major effect on B cells by TIF1γ loss. It is noticeable that the B-cell phenotype is similar to that of E2A-and Lyl1-difficient mice(Capron et al., 2006; Lazorchak et al., 2006). Interestingly, both E2A and Lyl-1 were found to form protein complexes with TIF1γ in K562 cells in our previous study(Bai et al., 2010). Whether TIF1γ predominantly regulates B-cell development through interaction with these proteins or has an independent role remains to be elucidated.

In contrast to the reduction of erythroid and B cell lineages, the increase of myeloid cells in TIF1γ-deficient mice suggests a negative role of TIF1γ in regulating this lineage. Loss of TIF1γ leads to a significant increase in myelopoiesis starting from the GMP stage and eventually progresses to a myeloproliferative disorder. In the *moonshine* mutant zebrafish, we found a similar phenotype of increased definitive myeloid cells in 4-day old embryos (data not shown), suggesting an evolutionarily conserved function of TIF1γ in the myeloid lineage. A recent study by Aucagne et al (Aucagne et al., 2011) reported a decrease of TIF1γ expression in a subset of human CMML samples due to hypermethylation of *tif1γ* promoter, suggesting a tumor suppressor function of TIF1γ. At the molecular level, we found that TIF1γ-deficient GMPs up-regulate genes associated with the myeloid fate while down-regulating those associated with the erythroid fate. While we have demonstrated a transcription activator role of TIF1γ that promotes Pol II elongation on erythroid genes, the mechanism by which TIF1γ represses gene expression is yet to be identified. It remains possible that paused elongation on one set of genes could lead to enhanced elongation on other genes, directly or indirectly, resulting in a change of cell fate.

A recent study by Kusy et al(Kusy et al., 2011) reported a reduction of LT-HSCs in the absence of TIF1γ. In contrast, we have observed an increase in the frequency of phenotypic LT-HSCs using both Mx-cre and vav-cre-mediated deletion. A similar increase in LT-HSCs was also found in the fetal liver of *vav-cre; tif1γ*^{fl/fl} embryos (data not shown). Despite this increase in the frequency and number of phenotypic LT-HSCs, competitive transplantation studies revealed a cell-autonomous defect in HSC function in TIF1γ-deficient cells.

In conclusion, using conditional gene inactivation we have identified cell-autonomous roles for TIF1γ in multiple cellular compartments of murine hematopoiesis. The function of TIF1γ in regulating transcription elongation of erythroid genes is evolutionarily conserved. It will be interesting to test in the future if the same transcriptional elongation mechanism is also used to regulate the cell fate of other blood lineages.

Supplementary Material

Refer to Web version on PubMed Central for supplementary material.

Acknowledgments

References

Alarcon C, Zaromytidou AI, Xi Q, Gao S, Yu J, Fujisawa S, Barlas A, Miller AN, Manova-Todorova K, Macias MJ, Sapkota G, Pan D, Massague J. Nuclear CDKs drive Smad transcriptional activation and turnover in BMP and TGF-beta pathways. Cell. 2009; 139:757–769. [PubMed: 19914168]

Aucagne R, Droin N, Paggetti J, Lagrange B, Largeot A, Hammann A, Bataille A, Martin L, Yan KP, Fenaux P, Losson R, Solary E, Bastie JN, Delva L. Transcription intermediary factor 1 gamma is a tumor suppressor in mouse and human chronic myelomonocytic leukemia. The Journal of clinical investigation. 2011; 121:2361–2370. [PubMed: 21537084]

Bai X, Kim J, Yang Z, Jurynec MJ, Akie TE, Lee J, LeBlanc J, Sessa A, Jiang H, DiBiase A, Zhou Y, Grunwald DJ, Lin S, Cantor AB, Orkin SH, Zon LI. TIF1gamma controls erythroid cell fate by regulating transcription elongation. Cell. 2010; 142:133–143. [PubMed: 20603019]

Capron C, Lecluse Y, Kaushik AL, Foudi A, Lacout C, Sekkai D, Godin I, Albagli O, Poullion I, Svinartchouk F, Schanze E, Vainchenker W, Sablitzky F, Bennaceur-Griscelli A, Dumenil D. The SCL relative LYL-1 is required for fetal and adult hematopoietic stem cell function and B-cell differentiation. Blood. 2006; 107:4678–4686. [PubMed: 16514064]

Cheng B, Price DH. Properties of RNA polymerase II elongation complexes before and after the P-TEFb-mediated transition into productive elongation. J Biol Chem. 2007; 282:21901–21912. [PubMed: 17548348]

Choe SE, Boutros M, Michelson AM, Church GM, Halfon MS. Preferred analysis methods for Affymetrix GeneChips revealed by a wholly defined control dataset. Genome Biol. 2005; 6:R16. [PubMed: 15693945]

Dupont S, Zacchigna L, Cordenonsi M, Soligo S, Adorno M, Rugge M, Piccolo S. Germ-layer specification and control of cell growth by Ectodermin, a Smad4 ubiquitin ligase. Cell. 2005; 121:87–99. [PubMed: 15820681]

Emanuel PD. Juvenile myelomonocytic leukemia and chronic myelomonocytic leukemia. Leukemia : official journal of the Leukemia Society of America, Leukemia Research Fund, U.K. 2008; 22:1335–1342.

Guenther MG, Levine SS, Boyer LA, Jaenisch R, Young RA. A chromatin landmark and transcription initiation at most promoters in human cells. Cell. 2007; 130:77–88. [PubMed: 17632057]

He W, Dorn DC, Erdjument-Bromage H, Tempst P, Moore MA, Massague J. Hematopoiesis controlled by distinct TIF1gamma and Smad4 branches of the TGFbeta pathway. Cell. 2006; 125:929–941. [PubMed: 16751102]

Kim J, Kaartinen V. Generation of mice with a conditional allele for Trim33. Genesis. 2008; 46:329–333. [PubMed: 18543301]

Klinakis A, Lobry C, Abdel-Wahab O, Oh P, Haeno H, Buonamici S, van De Walle I, Cathelin S, Trimarchi T, Araldi E, Liu C, Ibrahim S, Beran M, Zavadil J, Efstratiadis A, Taghon T, Michor F, Levine RL, Aifantis I. A novel tumour-suppressor function for the Notch pathway in myeloid leukaemia. Nature. 2011; 473:230–233. [PubMed: 21562564]

Kuhn R, Schwenk F, Aguet M, Rajewsky K. Inducible gene targeting in mice. Science. 1995; 269:1427–1429. [PubMed: 7660125]

Kusy S, Gault N, Ferri F, Lewandowski D, Barroca V, Jaracz-Ros A, Losson R, Romeo PH. Adult hematopoiesis is regulated by TIF1gamma, a repressor of TAL1 and PU.1 transcriptional activity. Cell stem cell. 2011; 8:412–425. [PubMed: 21474105]

Lazorchak AS, Wojciechowski J, Dai M, Zhuang Y. E2A promotes the survival of precursor and mature B lymphocytes. J Immunol. 2006; 177:2495–2504. [PubMed: 16888011]

Muse GW, Gilchrist DA, Nechaev S, Shah R, Parker JS, Grissom SF, Zeitlinger J, Adelman K. RNA polymerase is poised for activation across the genome. Nat Genet. 2007; 39:1507–1511. [PubMed: 17994021]

Ogilvy S, Metcalf D, Gibson L, Bath ML, Harris AW, Adams JM. Promoter elements of vav drive transgene expression in vivo throughout the hematopoietic compartment. Blood. 1999; 94:1855–1863. [PubMed: 10477714]

Orkin SH, Zon LI. Hematopoiesis: an evolving paradigm for stem cell biology. Cell. 2008; 132:631–644. [PubMed: 18295580]

Paulson RF, Shi L, Wu DC. Stress erythropoiesis: new signals and new stress progenitor cells. Current opinion in hematology. 2011; 18:139–145. [PubMed: 21372709]

Peterlin BM, Price DH. Controlling the elongation phase of transcription with P-TEFb. Mol Cell. 2006; 23:297–305. [PubMed: 16885020]

Porayette P, Paulson RF. BMP4/Smad5 dependent stress erythropoiesis is required for the expansion of erythroid progenitors during fetal development. Developmental biology. 2008; 317:24–35. [PubMed: 18374325]

Ransom DG, Bahary N, Niss K, Traver D, Burns C, Trede NS, Paffett-Lugassy N, Saganic WJ, Lim CA, Hersey C, Zhou Y, Barut BA, Lin S, Kingsley PD, Palis J, Orkin SH, Zon LI. The zebrafish moonshine gene encodes transcriptional intermediary factor lgamma, an essential regulator of hematopoiesis. PLoS Biol. 2004; 2:E237. [PubMed: 15314655]

Ransom DG, Haffter P, Odenthal J, Brownlie A, Vogelsang E, Kelsh RN, Brand M, van Eeden FJ, Furutani-Seiki M, Granato M, Hammerschmidt M, Heisenberg CP, Jiang YJ, Kane DA, Mullins MC, Nusslein-Volhard C. Characterization of zebrafish mutants with defects in embryonic hematopoiesis. Development. 1996; 123:311–319. [PubMed: 9007251]

Reymond A, Meroni G, Fantozzi A, Merla G, Cairo S, Luzi L, Riganelli D, Zanaria E, Messali S, Cainarca S, Guffanti A, Minucci S, Pelicci PG, Ballabio A. The tripartite motif family identifies cell compartments. Embo J. 2001; 20:2140–2151. [PubMed: 11331580]

Venturini L, You J, Stadler M, Galien R, Lallemand V, Koken MH, Mattei MG, Ganser A, Chambon P, Losson R, de The H. TIF1gamma, a novel member of the transcriptional intermediary factor 1 family. Oncogene. 1999; 18:1209–1217. [PubMed: 10022127]

Wada T, Takagi T, Yamaguchi Y, Watanabe D, Handa H. Evidence that P-TEFb alleviates the negative effect of DSIF on RNA polymerase Independent transcription in vitro. Embo J. 1998; 17:7395–7403. [PubMed: 9857195]

Wu CH, Yamaguchi Y, Benjamin LR, Horvat-Gordon M, Washinsky J, Enerly E, Larsson J, Lambertsson A, Handa H, Gilmour D. NELF and DSIF cause promoter proximal pausing on the hsp70 promoter in Drosophila. Genes Dev. 2003; 17:1402–1414. [PubMed: 12782658]

Yamaguchi Y, Inukai N, Narita T, Wada T, Handa H. Evidence that negative elongation factor represses transcription elongation through binding to a DRB sensitivity-inducing factor/RNA polymerase II complex and RNA. Mol Cell Biol. 2002; 22:2918–2927. [PubMed: 11940650]

Zeitlinger J, Stark A, Kellis M, Hong JW, Nechaev S, Adelman K, Levine M, Young RA. RNA polymerase stalling at developmental control genes in the Drosophila melanogaster embryo. Nat Genet. 2007; 39:1512–1516. [PubMed: 17994019]

Highlights

- TIF1γ plays essential and distinct functions in multiple hematopoietic lineages in mouse.

- TIF1γ is required cell-autonomously for murine hematopoiesis.

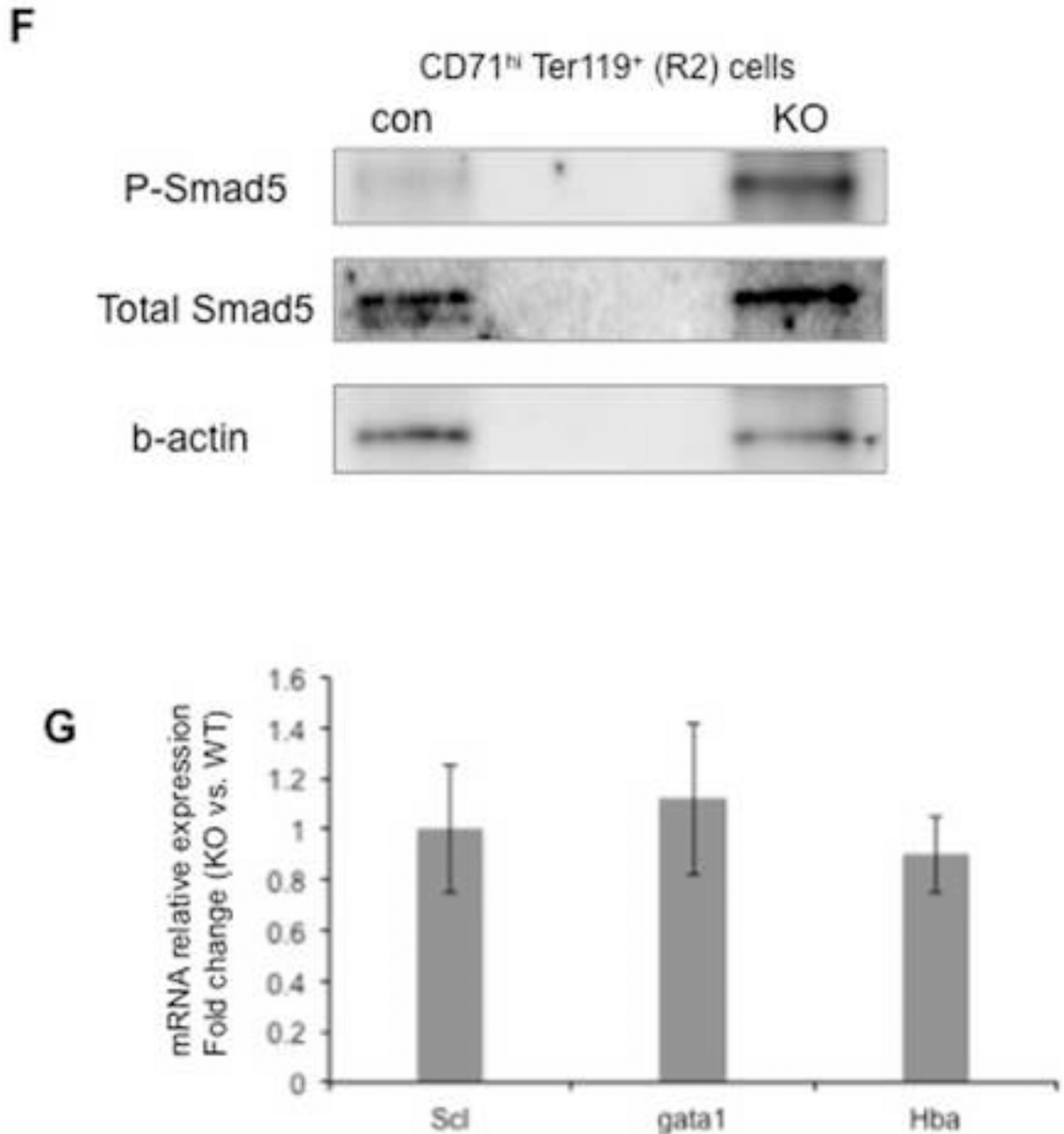- TIF1γ regulates the transcription elongation of murine erythoid genes.

F

G
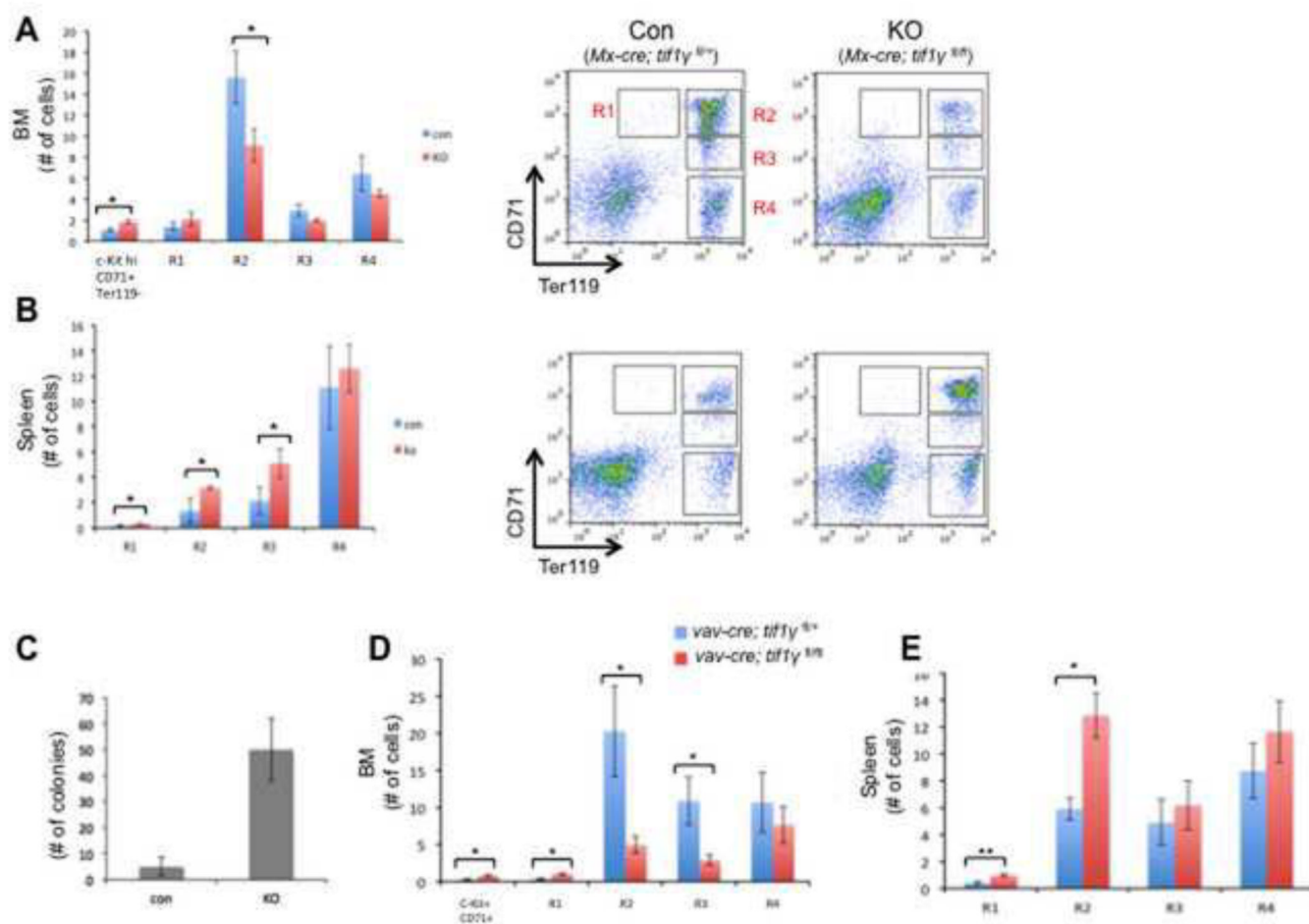
Figure 1. Abnormal erythropoiesis in TIF1γ-deficient mice
Erythroid cell maturation was measured by FACS based on the expression of the cell surface markers, c-Kit, CD71 and Ter119(Mx-cre for A&B, Vav-cre for D&E). The c-Kit^{hi}CD71$^+$ Ter119$^-$ cells represent the earlyerythroidprogenitors(see the cytospin staining in supplemental figure 1C). Populations R1-R4 represent the progressive maturation of cells. Bar graphs represent the absolute number of cells in each population. Representative FACS plots were shown in A&B. (A, D) Bone marrow cells. (B, E) spleen cells. The results are shown as mean ± SD from 3 or 4 mice in each group (* q 0.05, **q 0.005). (C) BFU-E colony assay using spleen cells from Mx-cre mice (n=3). The results are shown as mean ± SD. (F) Western blots comparing the protein level of phosphorylated Smad5 (top) and total

Smad5 (middle) in R2 cells between *vav-cre; tif1γ*^{fl/+} (con) mice and *vav-cre; tif1γ*^{fl/fl} (KO) mice. Western blot for b-actin was used as a loading control. The experiments were repeated twice using independent groups of mice. (G) Real-time RT-PCR analyses for selected erythroid genes in R2 stage of spleen erythroid cells from *vav-cre; tif1γ*^{fl/fl} (KO) mice and *vav-cre; tif1γ*^{fl/+} (con) mice. Results are shown as fold changes (KO vs. con), normalized to the level of b-actin. Error bars represent mean ± SD from three independent experiments.
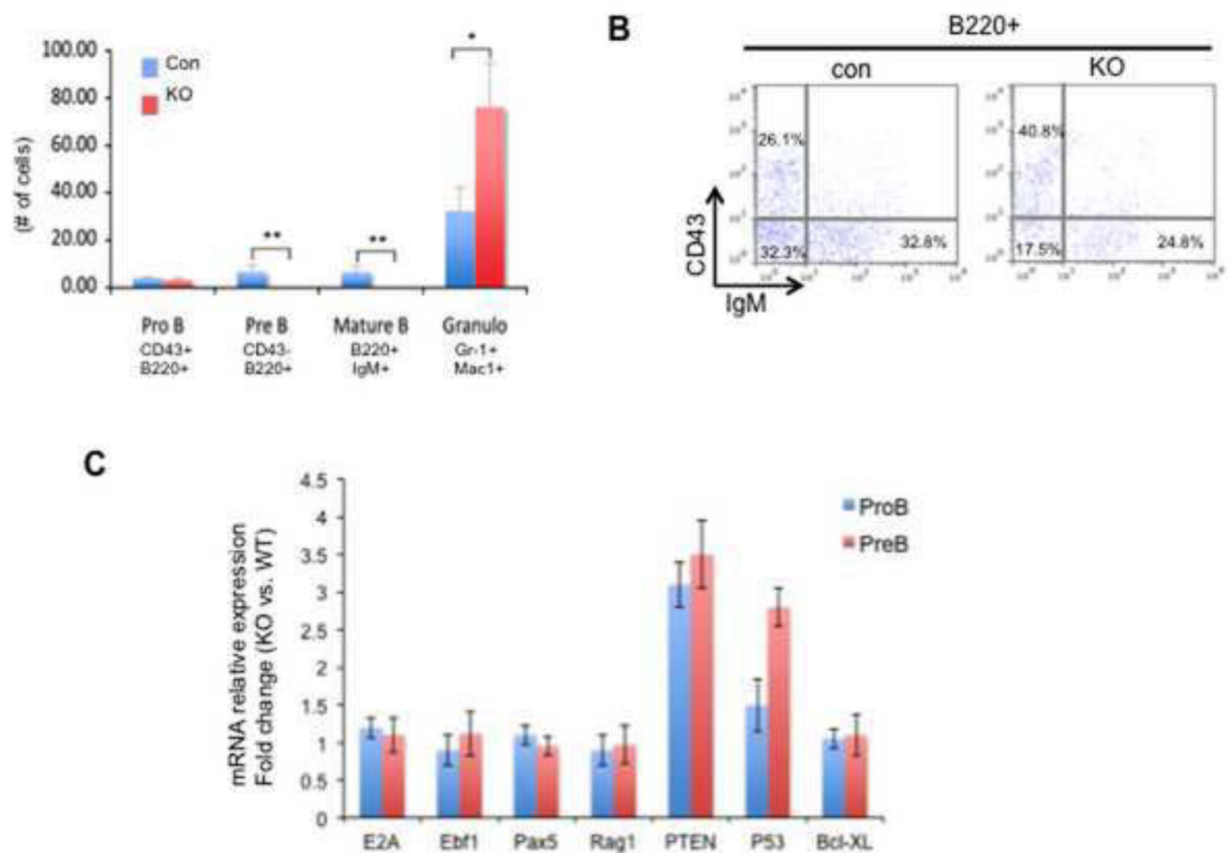
Figure 2. TIF1γ deficiency leads to loss of B cells
(A & B) Bone marrow cells from *Mx-cre; tif1γ*^{fl/+} (con) and *Mx-cre; tif1γ*^{fl/fl} (KO) mice were analyzed by FACS at 3-week post pI-pC injection. (A) The absolute numbers of cells in each population are shown. The results are shown as mean ± SD from 4 mice in each group (* q 0.01, ** q 0.001). (B) Representative FACS plots using B cell markers with the percentage of each cell population. (C) Real-time RT-PCR analyses for selected genes in pro-B and pre-B cells from *vav-cre; tif1γ*^{fl/fl} (KO) mice and *vav-cre; tif1γ*^{fl/+} (con) mice. Results are shown as fold changes (KO vs. con), normalized to the level of bactin. Error bars represent mean ± SD from three independent experiments.
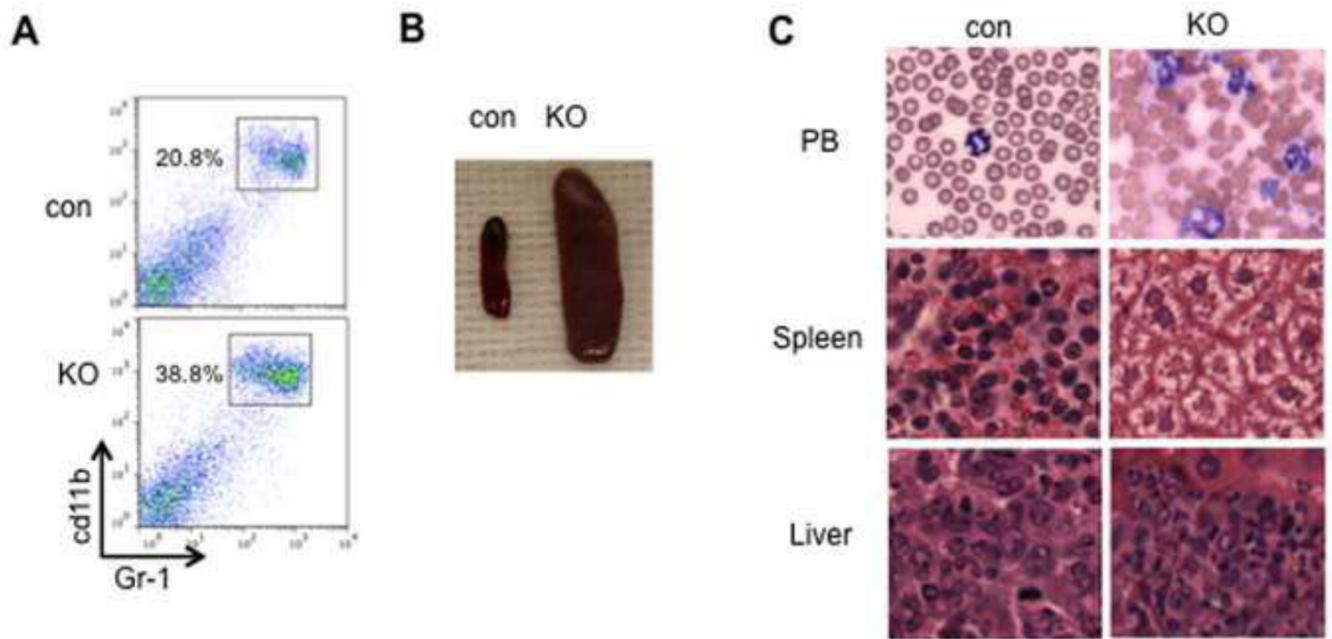
Figure 3. Accumulation of granulocytes in TIF1γ-KO mouse
(A) Representative FACS plots using myeloid cell markers with the percentage of each cell population. (B) Splenomegaly of 4-month old *vav-cre; tif1γ^{fl/fl}* (KO) adult mice (E) Accumulated myeloid cells in *vav-cre; tif1γ^{fl/fl}* adult mice in peripheral blood (PB, MGG staining), spleen and liver (H&E staining).
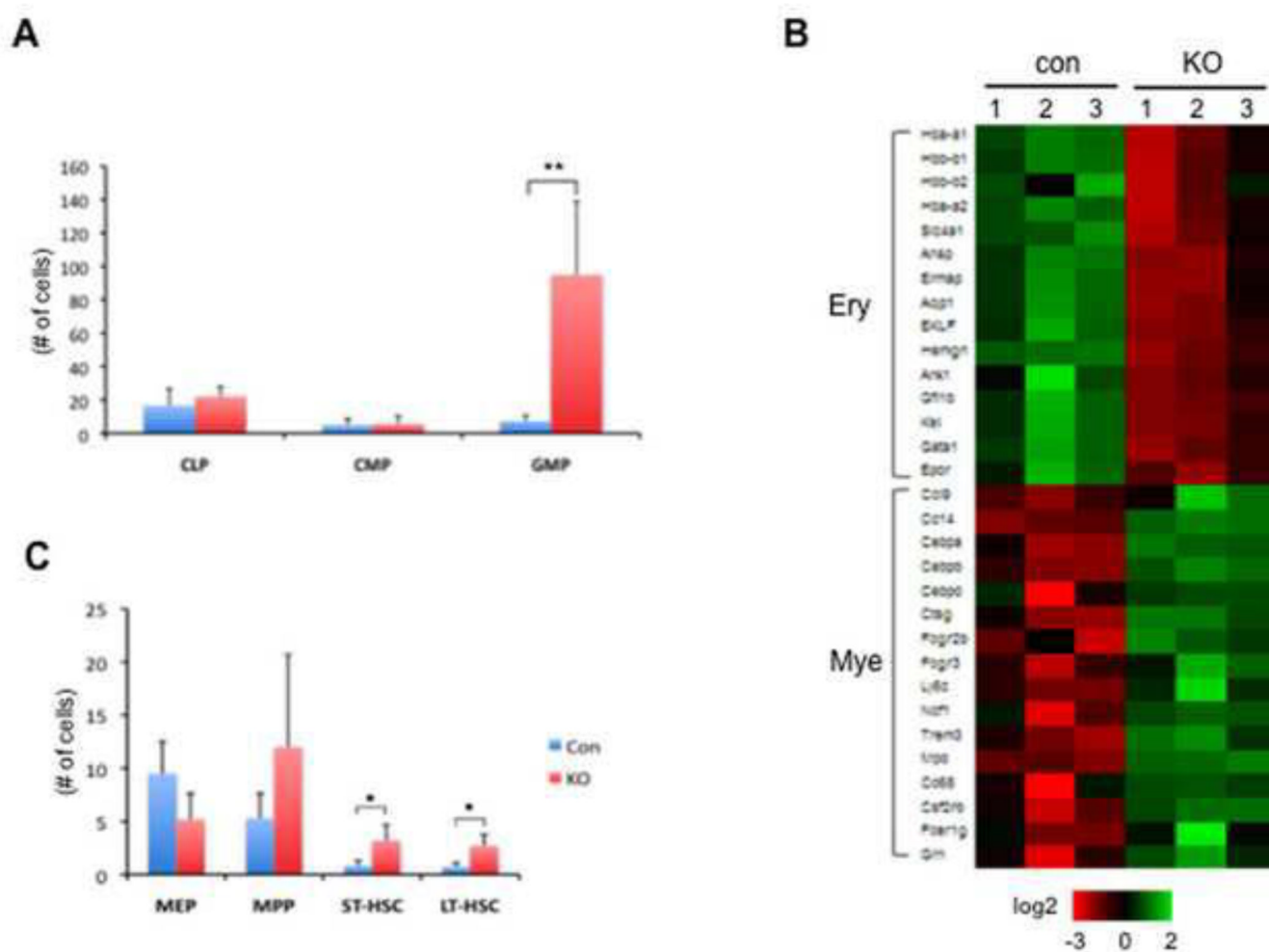
Figure 4. TIF1γ deficiency promotes myelopoiesis while inhibiting erythropoiesis
(A) Increased number of GMPs in *vav-cre; tif1γ*^{fl/fl} mice at 3-month old. The absolute
numbers of cells are shown as mean ± SD from 4 mice in each group (** q 0.001).
(B) Heat map showing regulation of genes representative of the erythroid signature and the
myeloid signature from GMPs derived from *vav-cre; tif1γ*^{fl/+} (con) and *vav-cre; tif1γ*^{fl/fl}
(KO) mice.
(C) Increased HSC levels in *vav-cre; tif1γ*^{fl/fl} mice at 3-month old. The absolute numbers of
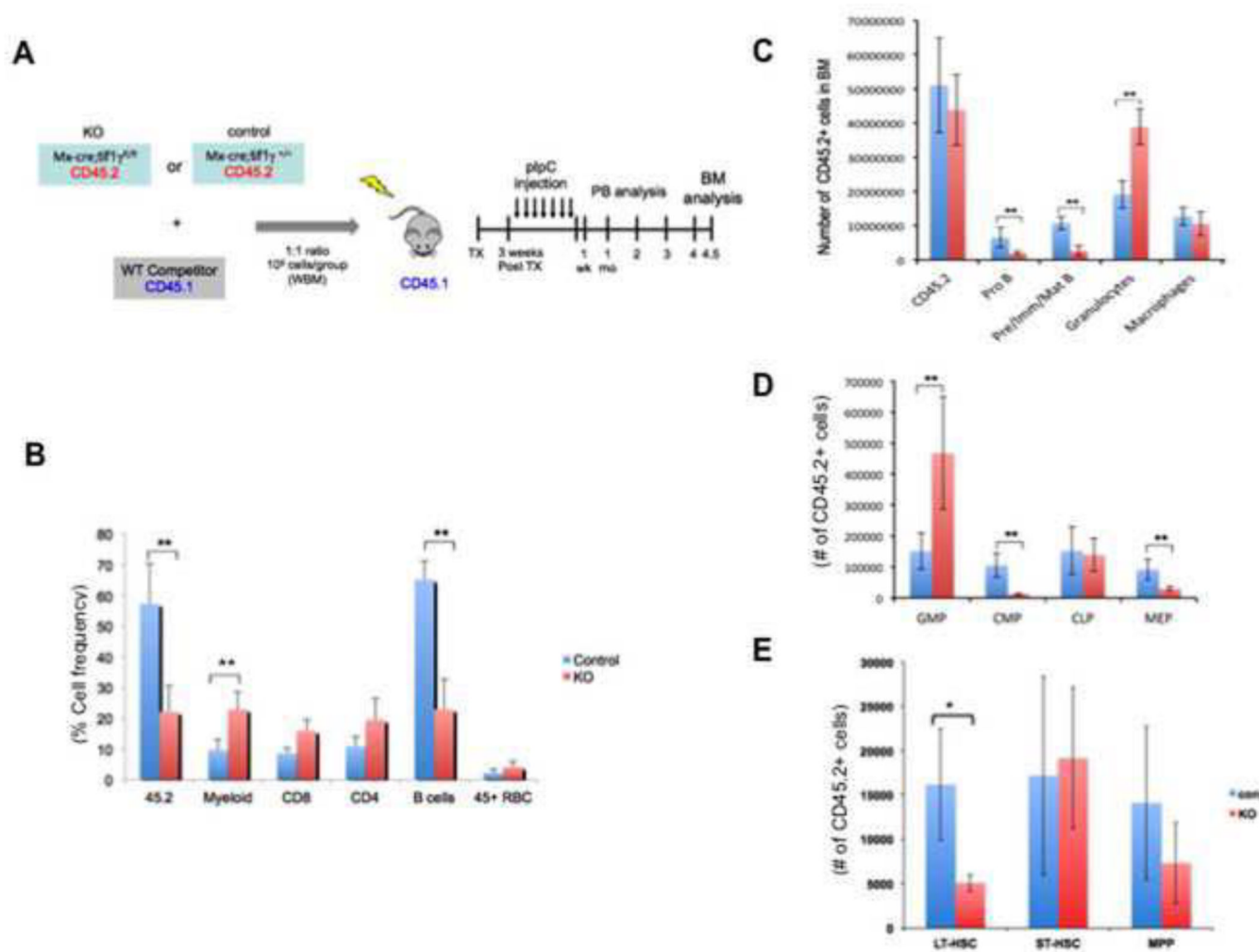cells are shown as mean ± SD from 4 mice in each group (* q 0.05).

Figure 5. TIF1γ has cell-autonomous functions in the regulation of hematopoiesis
(A) Scheme of the competitive transplantation assay
(B) Percentage of CD45.2$^+$ cells in the peripheral blood of recipients one-week after pI-pC injection. The results are shown as mean ± SD from 9 mice in each group (** q   0.001).
(C, D & E) FACS analyses to measure the numbers of CD45.2$^+$ cells in each cell population of the recipient bone marrow at 18-week post pI-pC injection. The results are shown as mean ± SD from 4 mice in each group(* q   0.01, ** q   0.001).
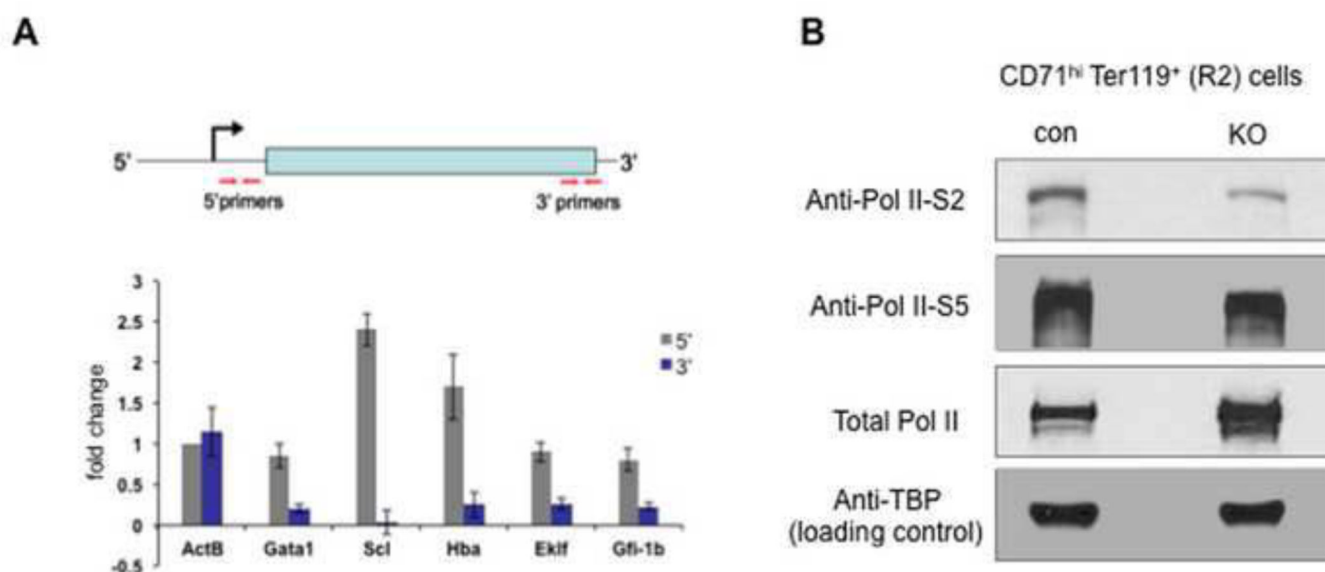
Figure 5. TIF1γ regulates the transcription elongation of erythroid genes
(A) Quantitative (real-time) RT-PCR comparing the transcription levels of selected genes in R2 stage of erythroid cells between *vav-cre; tif1γ*$^{fl/fl}$ (KO) mice and *vav-cre; tif1γ*$^{fl/+}$ (con) mice. **Top:** A schematic diagram showing the position of primers used in real-time RT- PCR analyses. Primers to detect the 5' ends of transcripts are located within 120bp from transcription start site, and primers for the 3' ends of transcripts are in the 3' coding region or 3'UTR. **Bottom:** real-time RT-PCR analyses to compare the 5' transcripts (gray) and 3' transcripts (blue). Results are shown as fold changes (KO vs. con), normalized to the ratio of the 5' transcript level of β-actin (ActB). Error bars represent mean ± SD from three independent experiments. Also see Supplemental Figure 4.

(B) Western blots comparing the protein level of serine 2-phophoralated Pol II (top), serine 5-phophoralated Pol II (middle) and total Pol II in R2 cells between *vav-cre; tif1γ*$^{fl/+}$ (con) mice and *vav-cre; tif1γ*$^{fl/fl}$ (KO) mice. Cells were pooled from 2 mice in each group. Western blots for the TATA binding protein (TBP, bottom) was used as a loading control. The experiments were repeated twice using independent groups of mice.